

Theoretical Study of the Quadruple Gamma Transitions of Radioactive Radon and Radium Isotopes Based on Half-Life

Duaa Abed Salim ^{a, }, Waleed Jabbar Mhana ^{a, }, Hadeel Ghali Ishnayin ^{a, }, and Khalid Hadi Mahdi ^{b, }

^aDepartment of Physics, College of science, Mustansiriya University, Baghdad, Iraq

^bDepartment of Physics, Faculty of Science, Karabuk University, Karabuk, Turkey

CORRESPONDANCE

Duaa Abed Salim
duaa.a.salim@uomustansiriyah.edu.iq

ARTICLE INFO

Received: April 04, 2024

Revised: September 02, 2024

Accepted: September 18, 2024

Published: December 30, 2024



© 2024 by the author(s).
Published by Mustansiriya University. This article is an Open Access article distributed under the terms and conditions of the Creative Commons Attribution (CC BY) license.

ABSTRACT: Background: This study investigated multiple aspects of radon and radium's nuclear properties since they are heavy, radioactive elements that may emit alpha, beta, and gamma radiation, which is connected to cancer and poses a risk to the environment. The purpose of this study is to investigate the significance of quadruple gamma transitions with $|M(E_2)|_{w.u.}^2$ as a valuable probe of the internal structure, deformations, and energy levels of atomic nuclei. **Objective:** By studying these gamma transitions, we hope to get more insight into the behavior of protons and neutrons within the nucleus as well as the fundamental forces governing their interactions. **Methods:** We applied MATLAB software to compute the probability of quadruple gamma transitions while accounting for the isotope energy characteristics and nuclei half-lives. **Results:** Our study's important results about the transition forces for particular isotopes are as follows: Ra-226 was reported to have the lowest transition force value, measuring 9.6623×10^{-17} , with a half-life of 1600 years. Furthermore, several transition force values were observed for Rn-214, the greatest values being 1.0248×10^4 and 1.5666×10^{-15} . On the other hand, Rn-216 has the highest recorded transition force value (1.70305×10^{-4}). **Conclusions:** The widths of Weisskopf transitions, gamma-gamma transitions, and gamma transitions were found by gathering and evaluating previously studied globally publicly available information. In the end, we successfully determined a relationship between the decay constant and the half-life of a decay event, which let us determine the probability that such events will occur within a certain time frame. Our study provides important insights into the transition probability within the examined nuclides and is in excellent agreement with global results and experimental data.

KEYWORDS: Radium; Radon; Quadruple transitions; Gamma ray; Gamma transitions

INTRODUCTION

The enigmatic quaternary gamma transitions of radioactive radon and radium isotopes invite us to take an exciting theoretical trip in nuclear physics. Based on the concept of half-life, this research could lead to significant discoveries that change our knowledge of atomic processes and decay [1]. We examine the depths of atomic science and use the power of time to reveal the secrets of radon and radium isotopes by deciphering their complex gamma transitions. Naturally occurring radioactive materials (NORMs) are present with human radiation exposure [2]. Recently, there has been a lot of discussion about radon, a colorless, odorless, and tasteless radioactive noble gas that occurs naturally [3]. The three primary isotopes of radon that are found in nature are ^{222}Rn , ^{220}Rn , and ^{219}Rn . ^{226}Ra immediate ancestor is ^{222}Rn [4]. They both belong to the uranium ($4n + 2$) series. Since ^{220}Rn belongs to the thorium ($4n$) series, it is often referred to as thoron (Tn). The isotopes of radon are all NORMs. However, ^{222}Rn and ^{220}Rn account for the majority of the radioactivity in the atmosphere at sea level. This is the convention that is then used ^{222}Rn [5], [6].

The existence of radiation that could be dangerous to human health is one of the biggest issues affecting the environment [7]. Gamma rays and other electromagnetic waves, such as alpha and beta particles, are two types of energy that can be transported across space or a physical medium. These types of energy are referred to as radiation [8]. Artificial (medical, fertility, mining, etc.) and natural (terrestrial and cosmic radionuclides) sources of radiation are both sources of internal and exterior radiation exposure for humans [9].

Inhaling airborne contaminants or consuming food and water polluted with radionuclides which may be alpha, beta, or gamma in nature leads to internal exposure, whereas external exposure results from the gamma decay of primordial radionuclides [10]. This problem statement emphasizes the urgent requirement to thoroughly comprehend, monitor, and control the various sources of radiation exposure and their associated health effects. It is imperative to tackle this problem to protect human health, the environment, and our collective future [11].

The significance of radon gas, which is formed by the disintegration of radium, which is a result of alpha dissolution, is to investigate the transmission of gamma rays [12]. Therefore, it is important to be aware of any additional dissolutions. As a result, it was investigated how gamma was transmitted from the second level to the ground level. Given that radon gas has been linked to lung cancer and that its chemical precursors, such as uranium, thorium, and radium, can be found in soil, water, and building materials, recent studies have highlighted the risk that radon gas poses to human health and safety [13]. Therefore, it is essential to take the required precautions to protect against the risk of gamma rays inherent in such research laboratory components, and attention must be paid to the security of researchers and lab personnel. In this section, we will provide an overview papers which searched for a topic. Aftab A *et al.*, in 2020 studied the implication of radon monitoring for earthquake surveillance using statistical techniques. A case study of the Henchman earthquake. Most of the statistical analysis is comprised of residual ^{222}Rn analysis employing a criterion of anomaly selection with a confidence interval of 95% and deterministic analysis of the Rn data. The Rn time series has a consistent trend ($0.5 \leq H \leq 1$), according to the deterministic analysis, which supports the lack of a chaotic regime. On the other hand, the response of distant monitoring stations to this specific earthquake ($R_E/R_D \geq 0.3$) further supports the association between Rn and seismic activity [14]. In addition, Jassim, F.A. *et al.*, 2011 studied the electric quadruple transition (E_2) in ^{56}Ba and ^{62}Sm nuclei in 2011, the transition strengths $|M(E_2)|_{w.u.}^2 \downarrow$ for gamma transition from first excited 2^+ states to the ground states that are produced by pure electric quadruple emission in even-even isotopes of ^{56}Ba and ^{62}Sm have been studied through half-lives time for 2^+ excited states with the intensities of 0^+ transition measurements and calculated as a function of neutron number. The outcomes obtained have demonstrated that nuclides like $^{56}\text{Ba}_{138}$ and $^{62}\text{Sm}_{144}$ that have magic neutron numbers have a minimal value for $|M(E_2)|_{w.u.}^2 \downarrow$ [15]. Moreover, researchers Rodellas *et al.*, measured groundwater and pore water flows to coastal and freshwater systems in 2021 using radium and radon isotopes, which are frequently studied as tracers. Specifically taken into consideration were conceptual uncertainties related to diffusive fluxes, radon escape into the environment, concentration of detectors, and changes in detector stock over time. According to the study, conceptual uncertainties should be considered when employing tracer mass balances because they are typically a significant source of uncertainty when predicting groundwater or porewater flows. The present research offers a pragmatic methodology for assessing the principal uncertainties linked to mass balances of radon and radium [16]. Furthermore, Vardaki *et al.*, are eager to get things done in 2021. Exosomal transcriptome analysis of plasma from 25 patients receiving radium-223 treatment as well as from our preclinical models (MDA-PCa 118b and TRAMP-C2/BMP4 PCa tumors). Every sample was tested twice, and $P < 0.05$ and fold changes of $+2$ to -2 were used to assess the array data. Tumor-derived genes and the tumor-associated bone microenvironment (bTME) are shown to be differentially enriched in plasma exosomes following radium-223 treatment, according to preclinical models. Exosomes made from plasma from patients receiving radium-223 showed comparable outcomes. These preclinical investigations showed that ICT can be utilized to boost the efficacy of ^{223}Ra and that RNA profiling of plasma exosomes can be used to track bTME's response to therapy [17]. Also in 2022, studies by researchers Riudavets *et al.*, demonstrated that alpha-ionizing radiation, which is released by radon radiation, has been connected to numerous cytotoxic and genotoxic effects. From a genetic perspective, the connection between radon and lung cancer is still poorly understood. Recent research has discovered the genetic changes that drive non-small cell lung cancer (NSCLC), particularly in the non-smoking population. These changes include chromosomal rearrangements (ALK, ROS1, RET, NTRK) and somatic mutations (EGFR, BRAF, HER2, MET). As of now, the risk factor is unknown. It has been suggested that non-smokers may be at risk for non-small cell lung cancer due to radon exposure. This study on indoor radon's effects on lung cancer carcinogenesis is useful, succinct, and current. It

highlights the gas's possible connection to non-small cell lung cancer (NSCLC) and its role in causing genetic abnormalities [18]. The previous studies have mostly focused on assessing the properties of radium and radon gas, largely from a radiological standpoint, with a specific emphasis on statistical and practical factors. The emphasis on this matter arises from the existence of alpha particles and the corresponding computations of alpha-ray radioactivity. Sadly, the existing literature lacks sufficient focus on the investigation of gamma-ray radioactivity, disregarding its practical, statistical, and theoretical dimensions. Therefore, it is vital to perform theoretical calculations to clarify the existence of gamma rays in these isotopes.

MATERIALS AND METHODS

This section will cover both the theoretical approach that was used in the calculations and the process that was utilized to extract the parameters for the gamma-ray quadruple transitions. A theoretical approach within the context of nuclear and atomic physics was used to calculate quadrupole transitions of gamma rays from an upper energy level to a lower energy level. An electromagnetic transition known as a quadruple transition occurs when the angular momentum of the nuclear or atomic system changes by two units ($\Delta J = 2$). Both atoms and atomic nuclei can undergo these changes, which are usually detected in gamma-ray spectroscopy.

The following procedures are commonly included in the theoretical method to compute gamma-ray quadruple transitions:

Data collection: The energy and half-lives of the isotopes were used to gather data for theoretical computations, in addition to obtaining data for algorithms that data lost objects [19].

The Transition Operator is computed: This operator represents the electromagnetic coupling responsible for the quadruple transition. The conversion factor is dependent on the type of response. The ratio of experimental gamma width to gamma width in Weisskopf units is the definition of the γ -ray transition strength $|M(\text{or } M, L)|_{w.u.}^2$. The strength of transition for γ -ray $|M(E \text{ or } M, L)|_{w.u.}^2$ written in eq. 1 [20], [21]:

$$|M(E \text{ or } M, L)|_{w.u.}^2 = \frac{\Gamma(E \text{ or } M, L)_{exp}}{\Gamma(E \text{ or } M, L)_{w.u.}} \quad (1)$$

If the gamma decay's overall width is [22]:

$$\Gamma_{\gamma} = \sum \Gamma_{\gamma l} \quad (2)$$

T is the mean lifetime of the original level, $\Gamma_{\gamma l}$ is the partial gamma width [23]:

$$\Gamma = \frac{\hbar}{T} \quad (3)$$

Where:

$$\Gamma_{\gamma} T \approx \hbar \quad (4)$$

Since:

$$\Gamma_{\gamma} T = 0.658212 \times 10^{-15} eV.s \quad (5)$$

Where Γ_{γ} is the total width.

The mean of a lifetime is [23], [24]:

$$T = \frac{t_{1/2}}{\ln 2} \quad (6)$$

$$\hbar = \frac{h}{2\pi} = 0.658212 \times 10^{-15} eV.s \quad (7)$$

The Plank constant is h [25]. For γ -transitions with mixed multi-polarities L and $L+1$, the total gamma width becomes [26]:

$$\Gamma_{\gamma} = \Gamma(L) + \Gamma(L+1) \quad (8)$$

Multi-pole Mixing Ratios (δ): Several theoretical and experimental studies have focused on the analysis of multi-pole mixing ratios (δ) of γ -rays emitted from excited nuclear states. In experiments, measurements of the angular distribution are the primary source of δ -values [27].

$$\delta^2 = \frac{t_{1/2}(\gamma) L}{t_{1/2}(\gamma) L + 1} \quad (9)$$

The most precise results for comparing with theoretical estimates based on various nuclear models are obtained from measurements of the E_2/M_1 mixing ratios of γ -transitions in even-even nuclei, which have long served as crucial tests for nuclear models [28]. Then the ratio of multi-polarities mixing can be obtained from eq. (7, 8) [29]:

$$\delta^2 = \frac{\Gamma(L + 1)}{\Gamma(L)} \quad (10)$$

For a transition of a pure quadrupole or pure electric dipole, E_2 , $\delta = 0$, so:

$$\Gamma(E1) \text{ or } \Gamma(E_2) = \Gamma_\gamma \quad (11)$$

Recent developments in the methods of producing intense beams of unstable nuclei have allowed for the discovery of various unusual features in neutron-rich nuclei, such as megacity loss, through measurements of transition strength. Where equation (1) yields the following transition intensity for a pure E_2 transition [23], [30].

$$|M(E_2)|_{w.u}^2 \downarrow = \frac{\Gamma(E_2)_{exp}}{\Gamma(E_2)_{w.u}} \quad (12)$$

RESULTS AND DISCUSSION

The outcomes will be presented in this section. The six Tables in this work are listed in three steps as follows:

Results of Radium

The ^{86}Rn isotopes' nuclear parameters are shown in Table 1, which includes the atomic number (Z), mass number (A) and neutron number (N) that were determined by $N=A-Z$. Gamma energy in the excited state was extracted in electron volts, along with the mean of lifetime and half-life in unit seconds.

Table 1. Half-life and mean lifetime for first excited states of ^{88}Ra

Z	A	N	Present work		
			E_γ (KeV)	$t_{1/2}$ (s)	T (s)
	212	124	629.3	13	18.7550
	214	126	1382.4	2.46	3.5490
	216	128	688.2	182×10^{-9}	2.6257×10^{-7}
	218	130	389.1	25.6×10^{-6}	3.6933×10^{-5}
	220	132	178.47	18×10^{-3}	2.5969×10^4
88	222	134	111.12	38.0	54.8224
	224	136	84.373	316224	4.5621×10^5
	226	138	67.67	1.26144×10^{10}	7.2795×10^{10}
	228	140	63.823	0.63×10^{-9}	9.0890×10^{-10}
	230	142	57.4	558	8.0502×10^3
	232	144	97.7	250	360.6738

In Table 1, the mean of half-life was calculated based on the half-life in seconds, as it is considered one of the nuclear properties of nuclei, meaning that the proportion between them is direct. Therefore,

the value of the half-lives is considered the designation for the isotopes that distinguish them from other isotopes, as the mass number starts from 212 to 232, based on the existing data for this element.

The features listed in Table 1 were used to derive the data for Table 2. The transition probability $|M(E_2)|_{w.u.\downarrow}^2$, Weisskopf gamma, and the total gamma widths for ^{88}Ra isotopes are shown in Table 2.

Table 2. Transitional capabilities $|M(E_2)|_{w.u.\downarrow}^2$ Partial gamma widths of γ_0 - rays from the $2^+ \rightarrow 1^+$ in ^{88}Ra nuclides, total gamma widths

Z	A	Present work			
		E_γ (KeV)	Γ_{tot}	$\Gamma_{w.u}$	$ M(E_2) _{w.u.\downarrow}^2$
	212	629.30	3.5096×10^{-17}	5.9768×10^{-6}	5.8720×10^{-12}
	214	1382.4	1.8546×10^{-16}	3.0959×10^{-4}	5.9907×10^{-13}
	216	688.20	2.5068×10^{-9}	9.5847×10^{-6}	2.6155810^{-4}
	218	389.10	1.7822×10^{-11}	5.6059×10^{-7}	3.1791×10^{-5}
	220	178.47	2.5347×10^{-20}	1.1520×10^{-8}	2.2002×10^{-12}
88	222	111.12	1.2006×10^{-17}	1.0910×10^{-9}	1.1005×10^{-8}
	224	84.373	1.4428×10^{-21}	2.7866×10^{-10}	5.1775×10^{-12}
	226	67.670	9.0212×10^{-27}	9.3582×10^{-11}	9.6623×10^{-17}
	228	63.823	7.2420×10^{-7}	7.0664×10^{-11}	1.0248×10^4
	230	57.400	8.1764×10^{-20}	4.2066×10^{-11}	1.9437×10^{-9}
	232	97.700	1.8250×10^{-18}	6.0793×10^{-10}	3.0019×10^{-9}

In Table 2, Γ_{tot} was calculated from equation (5), and $\Gamma_{w.u}$ was also calculated. As a result, $|M(E_2)|_{w.u.\downarrow}^2$ was calculated, as we found that there is a discrepancy in the calculated values. We notice that the highest value is in isotope 228, which is equal to (1.0248×10^4) because it has a half-life (0.63×10^{-9}) , whereas the lowest value is For $|M(E_2)|_{w.u.\downarrow}^2$, it depends on the half-life of the isotope. The lowest value is (9.6623×10^{-17}) for the isotope 226 because the half-life of this isotope is (1.26144×10^{10}) . If there was a stronger gamma transition force in the nucleus, the half-life would be shorter. A magic neutron number allows for the minimal value of $\Gamma(E_2)$ to $\Gamma(E_2)_{w.u.}$ to be determined, allowing for the calculation of $|M(E_2)|_{w.u.\downarrow}^2$. Which is limited to even-even nuclides for the isotope of ^{216}Ra . Therefore, the value of the gamma width reaches (2.6155×10^{-4}) .

Results of Radon

In this section, the radon results will be presented in two Tables, the first Table which is the nuclear properties of Z, A, and N, as well as the half-life and energy of the ^{86}Rn isotopes, are listed in Table 3.

In Table 3, the theoretical properties of radon isotopes have been listed, which represent the atomic number, the specified mass numbers (204-228), and the half-life. The mean half-life of these isotopes was calculated in seconds, as this range of mass numbers was chosen based on the presence of gamma decays in these isotopes. Table 4 for ^{86}Rn nuclides demonstrates the calculations' results. $|M(E_2)|_{w.u.\downarrow}^2$ is the transition force. For ^{86}Rn , it is displayed as a function of the N.

The results are summarized in Table 4 and indicate that while the experimental values of the partial gamma width Γ_{tot} are smaller than those estimated in the Weisskopf unit $\Gamma_{w.u.}$, the nucleon number appears to be deviating from the magic neutron number. Therefore, the values of the quadruple transition forces for gamma are different, for the ^{214}Rn isotope, the number of neutrons is one of the magic numbers 128, so the width of gamma is greater compared to other isotopes, where its value is (1.6897×10^{-9}) , reproduce the minimum diffraction at the number of neutrons magical = 128 contained in the nuclei ^{214}Rn .

Table 3. Half-life and mean lifetimes for first excited states of ^{86}Rn

Z	A	N	Present work		
			E_γ (KeV)	$t_{1/2}$ (s)	T(s)
	204	118	542.9	74.4	107.3365
	206	120	575.3	340.2	490.8048
	208	122	635.80	1461	2107.7774
	210	124	643.80	8640	12464.8851
	212	126	1273.8	1434	2068.8246
86	214	128	694.70	0.27×10^{-6}	3.89527×10^{-7}
	216	130	461.90	45×10^{-6}	6.4921×10^{-5}
	220	134	240.98	55.6	80.2138
	222	136	186.21	330350.4	4.76594×10^{-5}
	224	138	63.550	6420	9262.1021
	228	142	60.600	65	93.7751

Table 4. Transitional capabilities $|M(E_2)|_{w.u.}^2 \downarrow$ Partial gamma widths of γ_0 -rays from the $2^+ \rightarrow 1^+$ in ^{86}Rn nuclides, total gamma widths

Z	A	Present work			
		E_γ (KeV)	Γ_{tot}	$\Gamma_{w.u.}$	$ M(E_2) _{w.u.}^2 \downarrow$
	204	542.9	6.13230×10^{-18}	2.71334×10^{-6}	2.2600×10^{-12}
	206	575.3	1.34110×10^{-18}	3.67305×10^{-6}	3.6511×10^{-13}
	208	635.8	3.12281×10^{-19}	6.13412×10^{-6}	5.0908×10^{-14}
	210	643.8	5.28059×10^{-20}	6.61372×10^{-6}	7.9842×10^{-15}
	212	1273.8	3.18161×10^{-19}	2.03088×10^{-4}	1.5666×10^{-15}
86	214	694.7	1.68979×10^{-9}	9.92210×10^{-6}	1.7030×10^{-4}
	216	461.9	1.01387×10^{-11}	1.30540×10^{-6}	7.7667×10^{-6}
	220	240.986	8.2058×10^{-18}	5.17116×10^{-8}	1.5868×10^{-10}
	222	186.211	1.38108×10^{-21}	1.44177×10^{-8}	9.5791×10^{-14}
	224	63.55	7.10659×10^{-20}	6.7552×10^{-11}	1.0520×10^{-9}
	228	60.6	7.01912×10^{-18}	5.4534×10^{-11}	1.2870×10^{-7}

Evaluation of Results

In this section, the results will be evaluated with experimental results. The $|M(E_2)|_{w.u.}^2 \downarrow$ values are converted to $B(E_2)e^2b^2 \uparrow$ values for comparison, and the current $B(E_2)e^2b^2 \uparrow$ values of the γ transitions in the ^{88}Ra and ^{86}Rn nuclides are compared to both the experimental and model values. The alternative theory is distinct. Table 5 for ^{88}Ra and Table 6 for ^{86}Rn respectively exhibit this comparison.

The present values of $B(E_2)e^2b^2 \uparrow$ are compared to those provided in reference (Raman) based on experimental, global best fit, asymptotic values (RMF), and finite-range model (FRDM). The current results and the others seem to behave well in all N regions and are relatively close to one another in the reference (Raman). Finally, the existing values support evaluating the values of the measured quadrupole shifts E_2 predicted by various theoretical models because they agree with the values of the global best fit and those of the experimental data. Figure 1 and Figure 2 show a comparison of the existing values of $B(E_2)e^2b^2 \uparrow$ with those reported.

Table 5. The predicted decreased transition probabilities $B(E_2)e^2b^2\uparrow$ values for ^{88}Ra nuclides are compared to those of experimental, theoretical, and global best-fit predictions

Theoretical value			Present work			Z
B(E) e^2b^2 RMF	B(E) e^2b^2 FRDM	B(E) e^2b^2 Global fit	B(E) e^2b^2	E(KeV)	A	
0.007	0.134	0.89	0.8999	629.30	212	
0.001	0.008	0.4	0.4071	1382.4	214	
0.003	0.008	0.8	0.8127	688.20	216	
0.053	0.05	1.41	1.4287	389.10	218	
0.383	1.627	3.1	3.0957	178.47	220	
0.580	2.784	4.9	4.9421	111.12	222	88
0.643	4.762	6.4	6.4700	84.373	224	
1.400	5.316	7.9	8.0193	67.670	226	
3.934	5.922	8.3	8.4529	63.823	228	
5.342	7.114	9.2	9.3442	57.400	230	
6.468	8.406	5.4582	97.70	232	

Table 6. The predicted decreased transition probabilities $B(E_2)e^2b^2\uparrow$ values for ^{86}Rn nuclides are compared to those of experimental, theoretical, and global best-fit predictions

Theoretical value			Present work			Z
B(E) e^2b^2 RMF	B(E) e^2b^2 FRDM	B(E) e^2b^2 Global fit	B(E) e^2b^2	E(KeV)	A	
0.536	0.75	1.01	1.0221	542.9	204	
0.174	0.197	0.95	0.9583	575.3	206	
0.045	0.07	0.85	0.8615	635.8	208	
0.005	0.071	0.83	0.8454	643.8	210	
....	0.42	0.4246	1273.8	212	
0.001	0.007	0.76	0.7737	694.7	214	86
0.005	0.007	1.14	1.1564	461.9	216	
0.515	1.851	2.16	2.1896	240.986	220	
1.198	3.019	2.78	2.8166	186.211	222	
2.579	4.48	8.2039	63.55	224	
....	8.5024	60.6	228	

The quantity of neutrons in the nucleus is one of several variables that affects the likelihood of gamma decay or gamma transfer from an excited nuclear state to the ground state. It's important to remember that this relationship is not straightforward or linear as shown in Figure 1, and that the nuclear structure and unique characteristics of the target nucleus are better at explaining how gamma decay behaves. The number of protons and neutrons in the nucleus affects a variety of nuclear properties, including energy levels, nuclear states, and electromagnetic transitions. This is the reason behind the rise in the value of the transition probability $B(E_2)e^2b^2\uparrow$ in nuclear physics as shown in Figure 2. Based on quantum mechanics, the nuclear shell model describes the structure and energy levels of the nucleus.

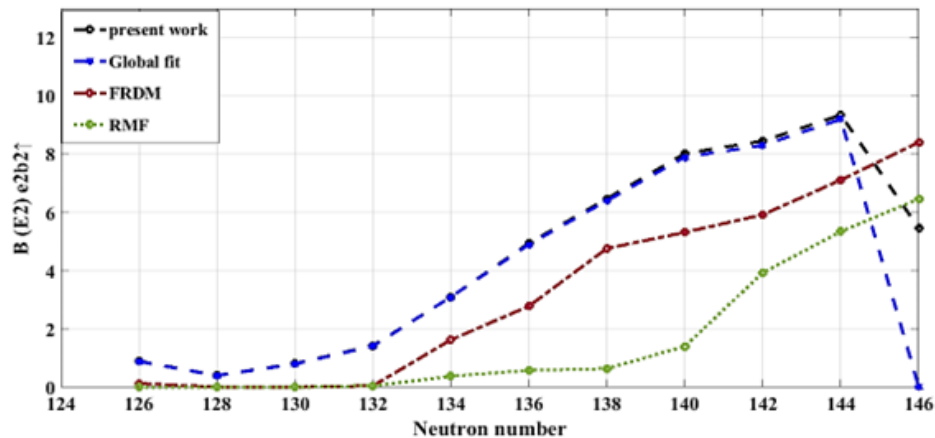


Figure 1. Comparison between the $B(E_2)e^2b^2\uparrow$ values of the present work for ^{88}Ra nuclides with global, experimental and other theoretical results

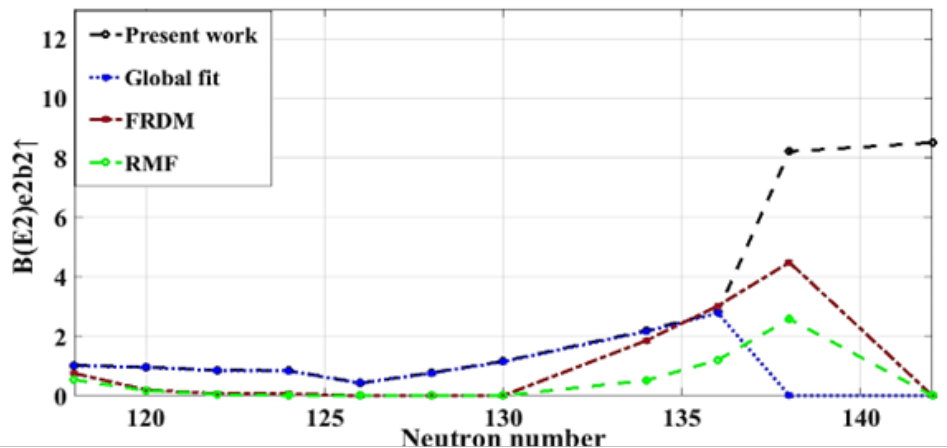


Figure 2. Comparison between the $B(E_2)e^2b^2\uparrow$ values of the present work for ^{86}Rn nuclides with global, experimental and other theoretical results

CONCLUSION

Radium and radon are heavy, radioactive elements that can produce alpha, beta, and gamma radiation, which is linked to cancer and poses a hazard to the environment, a variety of their nuclear properties were examined in this study. Since the behavior of some atomic nuclei is related to the transition of gamma radiation (γ), which includes a quadruple electrical transition $|M(E_2)|_{w,u\downarrow}^2$ dependent on the half-life of the isotopes, the gamma weisskopf and gamma widths were estimated to compute $|M(E_2)|_{w,u\downarrow}^2$. The analysis of radioactive isotopes and some alpha decays was the focus of earlier research; gamma decays and associated level transitions were not computed. We deduce from the tables in this study that the probability of the electrical quadruple transition $|M(E_2)|_{w,u\downarrow}^2$ is larger for nuclei with a magic number for one of the nucleons (protons or neutrons) than it is for other isotopes. Furthermore, since the values of $|M(E_2)|_{w,u\downarrow}^2$ rely on the nucleus' half-life and that relationship is inverse, we deduce that nuclei with long half-lives have lower values of $|M(E_2)|_{w,u\downarrow}^2$ than the other isotopes. We recommend that in addition to examining other transitions and the transitions of gamma from levels E_2, E_3 , and E_4 to the lower levels, researchers include the findings of this study in their future research.

SUPPLEMENTARY MATERIAL

None.

AUTHOR CONTRIBUTIONS

Duaa Abed Salima: Investigation, writing—review, and editing. Waleed Jabbar Mhana: Methodology, software. Hadeel Ghali Lshnayin: Formal analysis. Khalid Hadi Mahdi: Visualization and validation.

FUNDING

None.

DATA AVAILABILITY STATEMENT

None.

ACKNOWLEDGMENTS

We express our gratitude to Mustansiriyah University, specifically the College of Science and the Department of Physics, for their invaluable assistance.

CONFLICTS OF INTEREST

The authors declare no conflicts of interest.

REFERENCES

- [1] D. T. Esan, M. K. C. Sridhar, R. Obed, Y. Ajiboye, O. Afolabi, B. Olubodun, and O. M. Oni, "Determination of residential soil gas radon risk indices over the lithological units of a southwestern nigeria university," *Scientific Reports*, vol. 10, p. 7368, Apr. 2020. doi: 10.1038/s41598-020-64217-8.
- [2] M. A. Komorowski, "Radon and neoplasms," *Toxics*, vol. 11, no. 8, p. 681, 2023. doi: 10.3390/toxics11080681.
- [3] T. Davies, "A medical geology curriculum for african geoscience institutions," *Scientific African*, vol. 6, e00131, Nov. 2019. doi: 10.1016/j.sciaf.2019.e00131.
- [4] N. Majumder and S. Ghosh, "3d biofabrication and space: A 'far-fetched dream' or a 'forthcoming reality'?" *Biotechnology Advances*, vol. 69, p. 108 273, Dec. 2023. doi: 10.1016/j.biotechadv.2023.108273.
- [5] A. Jumaa Ahmed and H. Saadi, "Gene therapy approaches," *Qubahan Academic Journal*, vol. 1, no. 1, pp. 52–56, 2021. doi: 10.48161/qa.j.v1n1a35.
- [6] C. Clement, M. Tirmarche, J. Harrison, D. Laurier, F. Paquet, E. Blanchardon, and J. Marsh, "Lung cancer risk from radon and progeny and statement on radon," *Annals of the ICRP*, vol. 40, no. 1, pp. 1–64, 2010. doi: 10.1016/j.icrp.2011.08.011.
- [7] A. S. Aliyu, A. Ismaila, A. M. Na'Inna, and A. Mohammed, "Measurement of radon concentration in soil samples of mazat and kafi-habu mining sites, plateau, nigeria," *FUDMA Journal of Sciences*, vol. 4, no. 4, pp. 295–301, 2021. doi: 10.33003/fjs-2020-0404-485.
- [8] A. Wojcik, "Reflections on effects of low doses and risk inference based on the unsear 2021 report on 'biological mechanisms relevant for the inference of cancer risks from low-dose and low-dose-rate radiation'," *Journal of Radiological Protection*, vol. 42, no. 2, p. 023 501, 2022. doi: 10.1088/1361-6498/ac591c.
- [9] T. Sombo, F. Bibi, and A. Tyovenda, "Measurement of natural radionuclides and radon gas concentration in surface soil samples within jalingo metropolis, north east nigeria," *Nigerian Annals of Pure and Applied Sciences*, vol. 4, no. 1, pp. 125–130, 2021. doi: 10.46912/napas.233.
- [10] B. Samaila and H. M. Tampul, "Determination of soil radioactivity and radiological hazard indices in nigeria, a review," *Savanna Journal of Basic and Applied Sciences*, vol. 3, no. 1, pp. 71–80, 2021. [Online]. Available: <https://www.sjbas.com.ng/single.php?journalId=118>.
- [11] L. Liu, X. Xu, J. Han, J.-M. Zhu, S. Li, L. Liang, P. Wu, Q. Wu, and G. Qiu, "Heavy metal(loid)s in agricultural soils in the world's largest barium-mining area: Pollution characteristics, source apportionment, and health risks using pmf model and cd isotopes," *Process Safety and Environmental Protection*, vol. 166, pp. 669–681, Oct. 2022. doi: 10.1016/j.psep.2022.08.061.
- [12] G. T. Yachiso, A. K. Chaubey, and B. Turi, "Measurements of natural radionuclide levels and hazards in the lega dembi gold mine, oromia, ethiopia," *Isotopes in Environmental and Health Studies*, vol. 59, no. 4-6, pp. 554–566, 2023. doi: 10.1080/10256016.2023.2273287.

- [13] F. Papenfuß, A. Maier, S. Sternkopf, C. Fournier, G. Kraft, and T. Friedrich, "Radon progeny measurements in a ventilated filter system to study respiratory-supported exposure," *The National Center for Biotechnology Information*, vol. 13, p. 10792, Jul. 2023. doi: 10.1038/s41598-023-37697-7.
- [14] A. Alam, N. Wang, G. Zhao, and A. Barkat, "Implication of radon monitoring for earthquake surveillance using statistical techniques: A case study of wenchuan earthquake," *Geofluids*, vol. 2020, pp. 1–14, Mar. 2020. doi: 10.1155/2020/2429165.
- [15] O. A. Muaffaq and A. A. Al-Rubaiee, "Energy levels and electromagnetic transition of 90-94mo nuclei using ibm-1," *University of Thi-Qar Journal of Science*, vol. 7, no. 2, pp. 149–152, 2020. doi: 10.32792/utq/utjsci/v7i2.733.
- [16] V. Rodellas, T. C. Stieglitz, J. J. Tamborski, P. van Beek, A. Andrisoa, and P. G. Cook, "Conceptual uncertainties in groundwater and porewater fluxes estimated by radon and radium mass balances," *Limnology and Oceanography*, vol. 66, no. 4, pp. 1237–1255, 2021. doi: 10.1002/lno.11678.
- [17] I. Vardaki, P. Corn, E. Gentile, J. H. Song, N. Madan, A. Hoang, N. Parikh, L. Guerra, Y.-C. Lee, S.-C. Lin, G. Yu, E. Santos, M. P. Melancon, P. Troncoso, N. Navone, G. E. Gallick, E. Efstathiou, S. K. Subudhi, S.-H. Lin, C. J. Logothetis, and T. Panaretakis, "Radium-223 treatment increases immune checkpoint expression in extracellular vesicles from the metastatic prostate cancer bone microenvironment," *Clinical Cancer Research*, vol. 27, no. 11, pp. 3253–3264, 2021. doi: 10.1158/1078-0432.ccr-20-4790.
- [18] M. Riudavets, M. Garcia de Herreros, B. Besse, and L. Mezquita, "Radon and lung cancer: Current trends and future perspectives," *Cancers*, vol. 14, no. 13, 2022. doi: 10.3390/cancers14133142.
- [19] S. Raman, C. W. Nestor JR, and P. Tikkanen, "Transition probability from the ground to the first-excited 2+ state of even-even nuclides," *Atomic Data and Nuclear Data Tables*, vol. 78, no. 1, pp. 1–128, 2001. doi: 10.1006/adnd.2001.0858.
- [20] S. J. Mohammed, A. K. Aobaid, and S. A. Ebrahiem, "Calculation of total stopping power of the radioactive isotopes of carbon-14 and florine-18 used to treat cancer patients," in *Technologies and Materials for Renewable Energy, Environment, and Sustainability: TMREES23Fr*, vol. 3018, AIP Publishing, 2023, p. 020032. doi: 10.1063/5.0172339.
- [21] I. M. Hassan, S. A. Ebrahiem, and R. S. A. Al-Khafaji, "Calculated the quadrupole electrical transmission| m (e2)| 2 wu↓ for even-even nuclides of strontium (78-100sr and 66-76ge)," in *Technologies and Materials for Renewable Energy, Environment and Sustainability: TMREES21Gr*, vol. 2437, AIP Publishing, 2022, p. 020114. doi: 10.1063/5.0094215.
- [22] F. Kondev, M. Wang, W. Huang, S. Naimi, and G. Audi, "The nubase2020 evaluation of nuclear physics properties," *Chinese Physics C*, vol. 45, no. 3, p. 030001, 2021. doi: 10.1088/1674-1137/abddae.
- [23] D. A. Salim and S. A. Ebrahiem, "Study of transition strength for two isotopes carbon and oxygen," in *AIP Conference Proceedings*, vol. 2437, 2022. doi: 10.1063/5.0094340.
- [24] S. M. Ibrahim, S. A. Ebrahiem, and A. B. Rhaiem, "Calculating of the electric transition forces and radii of even-even-nuclei of cadmium (100-12448cd) cd isotopes," *Ibn AL-Haitham Journal For Pure and Applied Sciences*, vol. 37, no. 2, pp. 217–225, 2024. doi: 10.30526/37.2.3468.
- [25] A. E., "Lifetime measurements in 112;110te and band termination and beyond in 157er," Ph.D. dissertation, University of Liverpool, 2003.
- [26] F. B. Brown and W. R. Martin, "Monte carlo methods for radiation transport analysis on vector computers," *Progress in Nuclear Energy*, vol. 14, no. 3, pp. 269–299, 1984. doi: 10.1016/0149-1970(84)90024-6.
- [27] M. M. Hamarashid, "Determination multipole mixing ratios and transition strengths of gamma rays from level studies of 93mo (p,n γ) reaction," *Journal of Physical Science and Application*, vol. 2, no. 7, pp. 253–257, 2012.
- [28] S. A. Abbas, S. H. Salman, S. A. Ebrahiem, and H. M. Tawfeek, "Investigation of the nuclear structure of some ni and zn isotopes with skyrme-hartree-fock interaction," *Baghdad Science Journal*, vol. 19, no. 4, p. 0914, 2022. doi: 10.21123/bsj.2022.19.4.0914.
- [29] H. R. Yazar, I. Uluer, V. Unaloglu, and S. Yasar, "The investigation of electromagnetic transition probabilities of gadolinium isotopes with the ibfm- model," *Chinese Journal of Physics*, vol. 48, no. 3, pp. 344–355, 2010.
- [30] N. T. Jarallah, "Quadrupole moment & deformation parameter for even-even 38sr (a=76-102) nuclide," *Energy Procedia*, vol. 157, pp. 276–282, Jan. 2019. doi: 10.1016/j.egypro.2018.11.191.